PROBABILISTIC RISK ANALYSIS FOR AIRCRAFT STRUCTURES WITH LIMITED IN-SERVICE DAMAGES

Min Liao*, Yan Bombardier*, and Guillaume Renaud*
*** Aerospace Structures, National Research Council Canada (NRC)**
min.liao@nrc-cnrc.gc.ca

Keywords: Risk analysis, probability of failure, damage tolerance analysis, CP-140

Abstract

This paper presents some recent results of NRC research on risk assessment for aircraft structures. First, this paper briefly reviews the Canadian Forces (CF) risk assessment requirements related to aircraft structural life assessment. Because the single flight probability of failure (SFPOF) (instantaneous failure rate) is an important parameter used in aircraft risk assessment, a critical review of different SFPOF definitions and calculations is presented. As the size of the CF aircraft fleet is relatively small, one common issue encountered during risk assessment is that only a limited number of in-service damage findings are available. Several methods are discussed for preparing input data, especially the initial crack size distribution (ICSD), from small samples for structural risk analysis. To demonstrate one of the in-service damage based methods, a risk analysis case study is presented, in which limited in-service damage findings were used to calculate the SFPOF at a wing location, in support of the CF risk-based decision-making on maintenance actions and the operational life limit.

1 Introduction

Risk-based approaches and tools have been widely adopted by the aircraft communities, especially by the military, to ensure aircraft availability and to reduce cost while maintaining structural safety. In the past decade, the Canadian Forces (CF) have introduced and revised the Record of Airworthiness Risk Management (RARM) process to manage technical and operational airworthiness for all CF aircraft [1]. The RARM process includes five steps for risk management, i.e., Hazard Identification, Risk Assessment, Risk Control, RARM Approval, and Risk Tracking.

In RARM, a key airworthiness risk index is defined in Fig. 1, which is measured by a product combing both Hazard Severity and Hazard Probability. Fig. 2 presents the criteria to define the Hazard Severity. For Hazard Probability (probability of occurrence of the hazard), both *qualitative* (defining a hazard probability as 'frequent', 'remote', 'extremely improbable', etc) and *quantitative* (defining a hazard probability as '10^{-3}', '10^{-5}', '10^{-8}', etc.) are defined in Fig. 3 and Fig. 4, which can be used for *qualitative* and *quantitative* risk assessment, respectively. In particular, the *quantitative* hazard probability levels are defined in Fig. 4 for all CF aircraft platforms including unmanned air vehicles and helicopters.

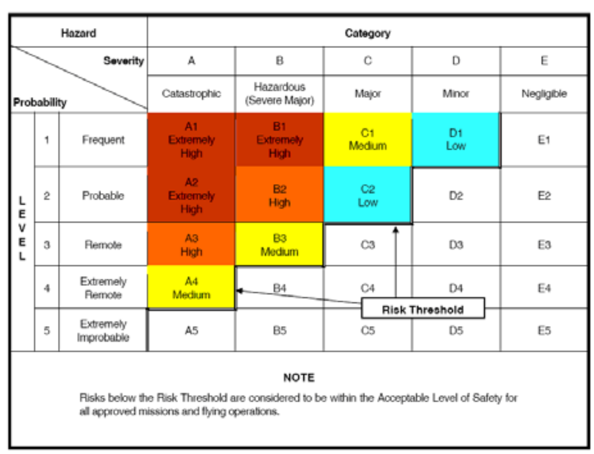

Fig. 1. CF airworthiness risk index [1]

Hazard Severity		Definition
Description	Category	
Catastrophic	A	All hazard conditions that would prevent continued safe flight and landing. Could result in death of the aircrew, normally with loss of the aircraft.
Hazardous (Severe Major)	B	Hazard conditions that would reasonably be expected to result in a large reduction in safety margins or functional capabilities, including higher aircrew workload or physical distress such that the aircrew may not be relied upon to perform tasks accurately or completely. Could result in death or major injury to aircraft occupants or major damage to an aircraft system. Could result in death or major injury to ground personnel or the general public.
Major	C	Hazard conditions that would reasonably be expected to result in a moderate reduction in safety margins or functional capabilities, including a moderate increase in aircrew workload or physical distress impairing crew efficiency. Possible physical distress, including injuries to occupants or minor damage to an aircraft system.
Minor	D	Hazard conditions that would not significantly reduce aircraft safety, but would reasonably be expected to result in a slight reduction in safety margins or a slight increase in aircrew workload.
Negligible	E	No effect on safety. Negligible effect on safety margins.

Fig. 2. Hazard severity [1]

Description	Level	Qualitative Definition	Life of Individual Aeronautical Product	Life of Entire Fleet	Individual Aircrew Career	All Exposed Personnel
Frequent	1	Likely to occur frequently.	Expected to occur frequently during the operational life of an individual aircraft.	Occurs continuously to the entire fleet.	Expected to frequently occur during an individual's career.	Occurs continuously to the entire population.
Probable	2	Expected to occur one or more times.	Expected to occur one or more times during the operational life of an individual aircraft.	Likely to occur several times per year to the entire fleet.	Expected to occur one or more times during an individual's career.	Likely to occur one or more times per year to the aircrew population.
Remote	3	Unlikely, but possible to occur.	Unlikely, but possible to occur during the operational life of an individual aircraft.	May occur one or more times per year to the entire fleet.	Unlikely, but possible to occur during an individual's career.	May occur one or more times per year to the aircrew population.
Extremely Remote	4	Not expected to occur.	Not expected to occur during the operational life of an individual aircraft.	May occur one or more times during the entire operational life of the entire fleet.	Not expected to occur during an individual's career.	May occur one or more times to the entire aircrew population.
Extremely Improbable	5	So unlikely, it may be assumed that it will never occur.	So unlikely, it may be assumed that it will never occur during the entire operational life of all aircraft of the type.			

Fig. 3. Qualitative hazard probability [1]

Hazard Probability Level	Hazard Probability Thresholds (Per Flight Hour)			
	DND Passenger Carrying Aircraft *(Derived from FAR 25/29 Civil Designs)*	Military Aircraft		
		Military Aircraft	Military Aircraft - *Ejection Seat Equipped*	Unmanned Aerial Vehicles (UAVs) * *Above 150Kg TOW*
Frequent	Greater than 1×10^{-3}	Greater than 1×10^{-3}	Greater than 1×10^{-2}	Greater than 1×10^{-2}
Reasonably Probable	Less than 1×10^{-3}	Less than 1×10^{-3}	Less than 1×10^{-3}	Less than 1×10^{-2}
Remote	Less than 1×10^{-5}	Less than 1×10^{-5}	Less than 1×10^{-4}	Less than 1×10^{-3}
Extremely Remote	Less than 1×10^{-7}	Less than 1×10^{-6}	Less than 1×10^{-5}	Less than 1×10^{-5}
Extremely Improbable	Less than 1×10^{-9}	Less than 1×10^{-8}	Less than 1×10^{-7}	Less than 1×10^{-6}

Fig. 4. Quantitative hazard probability [1]

Today, the RARM has become the single most critical decision making tool in the CF air fleet life-cycle management [2]. When there are sufficient data available, a *quantitative* risk assessment (RA) can be performed to substantiate the assignment of a risk index. When a *qualitative* RA indicates a high or medium risk, a detailed *quantitative* RA is often requested to calculate the hazard probability to gain additional confidence in decision-making.

The CF RARM process was designed to cover all the airworthiness and safety related aircraft systems including hydraulics, structural, mechanical, avionics, etc. For aircraft structural systems, the potential hazards include structural failures that can cause injury or death to personnel, damage to or loss of the aircraft, or reduction of mission readiness or availability. Since the majority of structural failures are due to fatigue fracture under both cyclic loading and environment-related aging, like corrosion, it is more difficult to carry out a *quantitative* risk analysis for aircraft structures due to its complexity. Further, there are a lot less structural failure data compared to other systems, and simple data-driven reliability or empirical statistical models may not be applicable for a structural risk analysis. Given that a damage tolerance analysis (DTA) is available for fatigue critical locations, a fracture mechanics based method is usually used for structural *quantitative* risk analysis.

To support the CF RARM process, especially for *quantitative* risk analysis, NRC has been developing structural risk analysis methods and tools in collaboration with Defence Research and Development Canada (DRDC). An in-house tool, ProDTA (Probabilistic Damage Tolerance Analysis), has been developed at NRC for structural risk analysis by taking into account both conventional fatigue damage and age-related environmental damage (i.e. corrosion) [3]. The NRC tool has been used for a number of risk analyses for different CF aircraft structures, including build-up structures containing multi-site fatigue damage (MSD) and multi-element damage (MED) [4]. This paper presents recent improvements of ProDTA and a risk analysis case study conducted using this tool based on limited in-service damage data.

2 Review of different SFPOF calculations

In structural applications, the CF uses the single *flight hour* probability of failure (SFHPOF) to represent the hazard probability of critical locations for the RARM process (Fig. 1 (b)). This is similar to the single flight POF (SFPOF)① used by the US Air Forces (USAF) Aircraft Structural Integrity Program (ASIP) MIL-STD-1530C [5], the Department of Defense (DoD) Joint Service Specification Guide JSSG 2006 [6], and MIL-STD-882D [7]. It should be noted that none of these high-level documents specify the statistical definition of the SFPOF, nor the mathematical procedures to calculate it. In the past, different SFPOF definitions have been used by different operators/users and sometimes the difference between the different SFPOFs could be several orders of magnitude. Recently, some detailed reviews and comparisons of several SFPOF definitions and calculations were carried out at NRC [8]. Some relevant results are summarized in this paper.

2.1 Lincoln and USAF SFPOFs

In 1985, Lincoln published a fracture mechanics based method to calculate the SFPOF [9] by assuming that at a given time the crack size distribution function is independent of the stress density function for a particular control point. The following equation is considered② to represent the Lincoln method for the SFPOF calculation at the i-th flight:

$$POF(i) = P\left[\sigma > \frac{K_c}{\alpha(a_i)}\right]$$
$$= \int_0^\infty f_i(a_i) \int_0^\infty g(K_c)\left[1 - H\left(\frac{K_c}{\alpha(a_i)}\right)\right] dK_c\, da_i \qquad (1)$$

where

$POF(i)$: POF at the i-th flight
σ: applied stress
K_c: fracture toughness
a_i: crack size at the i-th flight
$\alpha(a_i)$: stress intensity at a location divided by the applied stress, or $\beta(a)\sqrt{\pi a}$
$f_i(a_i)$: probabilistic density function (PDF) of the crack size a at the i-th flight
$g(K_C)$: probabilistic density function (PDF) of the fracture toughness K_C
$H(\sigma)$: distribution of the peak/maximum stress per single flight

In 1991, Berens used the Lincoln SFPOF definition in the USAF tool PROF (Probability of Fracture) V1.0 [10], and then modified Eq. (1) in PROF V2.0 for using a residual strength (RS) curve, $\sigma_{RS}(a)$, as a function of crack size,

$$POF(i) = P[\sigma > \sigma_{RS}(a)]$$
$$= \int_0^\infty f_i(a_i)[1 - H(\sigma_{RS}(a_i))]\, da_i \qquad (2)$$

In practice, the RS function $\sigma_{RS}(a)$ can be determined by taking the minimum stress from multiple failure criteria, including fracture toughness, net section yielding, and plastic zone linkup. In 2005, PROF V3.0 slightly revised Eq. (2), as an indirect way to calculate it as a hazard rate ($h(t)$), which actually calculates the SF<u>H</u>POF for the K_C and RS failure criteria [8].

2.2 Freudenthal SFPOF

It was recently rediscovered that Freudenthal and Shinozuka had developed comprehensive reliability methods in 1966 to calculate the hazard rate based POF considering *all* non-prior failure events. The Freudenthal equation for the SFPOF calculation is:

$$POF(i) = h(t_i) = \frac{f(t_i)}{1 - F(t_i)} \qquad (3)$$

where

① For a small probability (~1×10^{-7}), SFPOF ≅ SFHPOF × Number of hours per flight.

② Lincoln's original formula did not explicitly show all variables. PROF V1.0 presented them using the same SFPOF definition.

$$f(t_i) = \int_0^\infty g(K_c)\left\{\int_0^\infty f_0\,(a_0)\left[\prod_{j=1}^{i-1} H\left(\frac{K_c}{\alpha[a(a_0,t_j)]}\right)\right] * \left[1 - H\left(\frac{K_c}{\alpha[a(a_0,t_i)]}\right)\right] da_0\right\} dK_c \quad (4)$$

$$F(t_i) = \int_0^\infty g(K_c)\left\{\int_0^\infty f_0\,(a_0)\left[1 - \prod_{j=1}^{i} H\left(\frac{K_c}{\alpha[a(a_0,t_j)]}\right)\right] da_0\right\} dK_c \quad (5)$$

Note:

- For the RS failure criterion, Eqs (4-5) can be modified by replacing the $H\left(\frac{K_c}{\alpha(a_0,t_i)}\right)$ with $H[\sigma_{RS}(a)]$.
- For a very small probability (<10^{-7}), it was shown that $POF(i) = h(t_i) \cong f(t_i)$ [8].
- When the product or the probability of non-prior failure events $\prod_{j=1}^{i-1} H\left(\frac{K_c}{\alpha\left(a(a_0,t_j)\right)}\right)$ = 1.0, the Freudenthal Eq. (4) is the same as the Lincoln Eq. (1). Although this product could be very close to 1.0 for high reliability problem or at the early stage of aircraft usage, mathematically it should always be less than 1.0. Consequently, the Lincoln Eq. (1) should always gives higher (more conservative) POF results than the Freudenthal Eq. (3). Due to this product, the computation time for the Freudenthal equations is significantly increased.

In some cases such as the USAF risk analysis example published in [8], the POF difference between the Lincoln and Freudenthal equations could reach two orders of magnitude. In other cases, especially when using the residual strength failure criterion, there was virtually no difference until the POF became very high (e.g. 10^{-4} to 10^{-5}) [8].

Although Freudenthal and Shinozuka developed the exact reliability equations ($F(t)$, $f(t)$, $h(t)$), they were not used in their examples maybe due to the limited computing power in the 1960s. Alternatively, approximated equations were proposed and actually used in their examples.

2.3 NRC ProDTA SFPOF

In the past, the NRC in-house tool ProDTA used methods and equations similar to Lincoln and PROF for the SFPOF calculation. However, ProDTA uses different numerical integration subroutines, and is enhanced with Monte Carlo simulation on crack growth modeling. Recently, additional numerical integration subroutines were developed which allows ProDTA to calculate the Freudenthal exact reliability using Eqs. (4-5), as well as the SFPOF using Eq. (3).

The review and comparison of different SFPOF calculations supported the need to formally define a standard SFPOF in the controlled documents for aircraft structural risk analysis. To that end, more benchmark examples may be needed. From several numerical examples carried out in [8], it was verified that the Lincoln equations did give more conservative (higher) SFPOF than the Freudenthal equations, while the difference was reduced when a deterministic residual strength failure criterion was applied. In the case study presented in the following section, the Lincoln equation was used for the SFPOF calculation.

3 Risk analysis using limited in-service data

In a risk analysis, the SFPOF is calculated based on a crack size distribution $F(a)$ which is obtained from an initial crack size distribution (ICSD), using either a master crack growth curve or a Monte Carlo crack growth program. The ICSD is the most significant input for risk analysis. With a single or limited in-service damage findings, the determination of the ICSD becomes very challenging. In general, the following approaches may help determine an ICSD:

a) Use a single or limited in-service data together with historical data from a time-to-crack size (TTCS) distribution to determine an ICSD or an equivalent initial flaw size (EIFS) distribution. This ICSD/EIFSD would simply include all the scatters caused by the material, geometry, and load/usage of the aircraft components. It would be of high fidelity but would only represent the specific location or component for which it was developed.

b) Use damage data from a full scale fatigue test (FSFT) and teardown inspections to determine an ICSD. Given that the correlations between the individual aircraft usage and FSFT spectra are available, the FSFT data could be used in association with the in-service data described in the first method.

c) Use material initial discontinuity states (IDS) such as particles, pores, and manufacturing damages, based on the Holistic Structural Integrity Process (HOLSIP) supported by coupon test data. This case may also occur in the design stage of new aircraft using new material, or in the early service stage of a new aircraft. The material IDS can be applied to develop an initial discontinuity state distribution (ICSD), along with coupon fatigue test data. The IDS concept was first developed under the HOLSIP framework, which is still under development. Different from the EIFS, the IDS are physical features related to crack nucleation, growth, and failure. Physics-based models are needed to correlate the IDS with macro-cracks that can be detected in service. Since the IDS represents the overall material discontinuity population for all potential cracking features, including coupon and/or component tests, in-service damages can be used to narrow-down the IDS subset that are responsible for specific aircraft cracking. The Bayesian method may be used to narrow-down or update the IDS subset, which would lead to more accurate crack size distributions and risk analysis.

Depending upon the data available for the specific aircraft structures, different approaches may be applied. Some detailed description on the above approaches was documented in [11], along with case studies for the methods. In this paper, the in-service damage based approach was applied for a risk analysis case study of the CP-140 wing structure with only one, the first, damage finding.

3.1 Case study

Following some wing lower forward spar cap inspection results from the US Navy P3 fleet in 2007, the CF launched the RARM process and an initial *qualitative* risk assessment indicated that the CP-140 Aurora fleet (the Canadian version of the P3) was under a *high* risk when reaching the targeted operational lifetime (24,500 hours). As this risk analysis was solely based on the USN P3 findings and no CF inspections, the CF initiated a Canadian Special Inspection (CSI) line to inspect the affected wing areas in order to re-assess the risk level. Some wing structures were first removed from three CP-140 aircraft and sent to the Quality Engineering Test Establishment (QETE) for detailed inspections. In the meantime, NRC was requested by the CF to carry out some *quantitative* risk analysis to calculate the POFs of some critical locations in the CP-140 wing, including a location at the front spar cap aft flange at wing station (WS) 130, also referred to as Location 3 in this paper. The typical geometry and cracking paths of the critical locations between WS65 and WS167, including Location 3, are shown in Fig. 5.

3.2 Initial crack size distribution

For the spar cap between WS65 and WS167, the full scale fatigue test showed about 20 cracks and the USN P3 showed over 20 cracks only between WS90 and WS140. However, from the first three CF CP-140 aircraft inspected, only one “crack indication” was reported by QETE at Location 3 and adjacent holes within WS90-140, i.e., for total of 396 holes in three aircraft.

For a quick conservative risk analysis, this “indication” was assumed as a crack whose size was 0.030”, which represents $p^*=1/396$ or the 0.253th percentile in a crack size distribution.

This crack, along with the USN P3 in-service crack findings, was used to determine an EIFSD as follows:

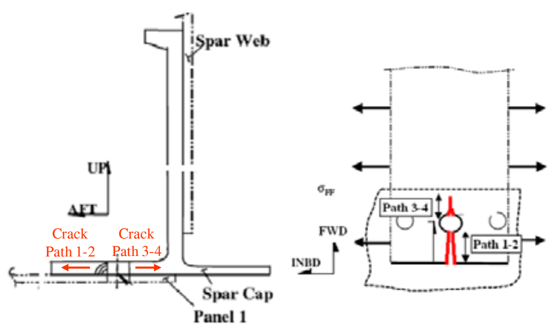

Fig. 5. Typical geometry and multi-phase cracking paths for critical locations within WS65-167, including Location 3 - front spar cap aft flange at WS130 (not to scale)

1) For the CF aircraft, it was assumed that the time to crack size (TTCS) distribution followed a Lognormal distribution that had the same standard deviation as that of the USN TTCS. Since the USN in-service findings were obtained at different times, the TTCS data were regressed to a common crack size of 0.03" using a master crack growth curve (described in Section 3.3), as shown in Fig. 6. Two standard deviations of the natural logarithmic TTCS data (log-TTCS) were calculated as 0.103, before TTCS regression, and 0.133 after TTCS regression. In total 28 cracks from the USN P3s were used in the analysis, and no null-findings (censored data) were used. Excluding the null-findings would make the PoF results more conservative.

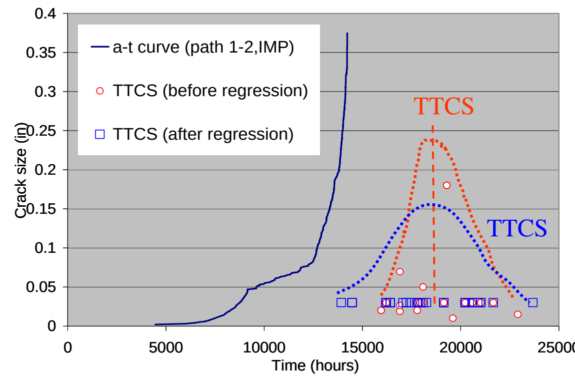

Fig. 6. USN TTCS distribution before and after the regression

2) Using the percentile of one crack finding (p*= 0.25%), the mean of the log-TTCS distribution for the CF aircraft was calculated as,

$$\mu_{\log-TTCS} = \ln(T^*) - \Phi^{-1}[p^*] \bullet \sigma_{\log-TTCS} \qquad (6)$$

where T^* is the inspection time for the CF aircraft, i.e. 22,162 hours, $\Phi^{-1}[p]$ is the inverse function of a standard Normal distribution, and $\sigma_{\log-TTCS}$ is the standard deviation of the log-TTCS distribution.

3) Using a master crack growth curve, the CF TTCS distribution was regressed to time zero to determine an EIFS distribution, as shown in Fig. 7. In this approach, a certain percentile p^* of crack was regressed to an EIFS but with $1-p^*$ percentile. Two EIFSDs were determined using $\sigma_{\log-TTCS}$ = 0.103 (before TTCS regression), and $\sigma_{\log-TTCS}$ = 0.133 (after TTCS regression), as presented in Fig. 8.

If more CF in-service cracks were available, a maximum likelihood method could be used to estimate the parameters of the TTCS distribution, with and without censored data (null-findings) [14].

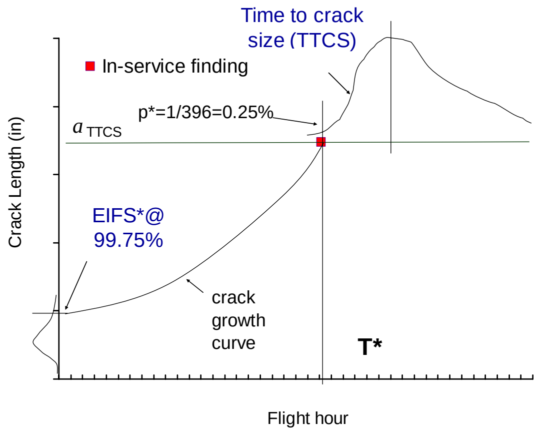

Fig. 7. Schematic of the regression of EIFSD from TTCS

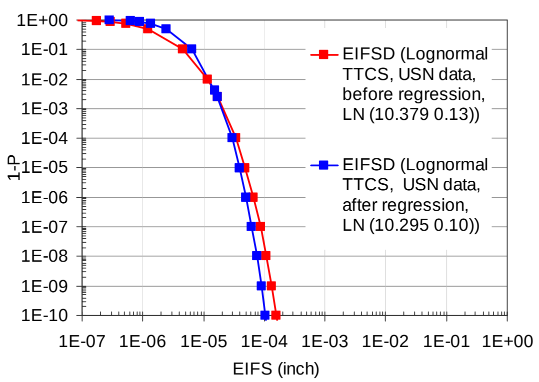

Fig. 8. EIFSDs for CP-140 Location 3, expressed as the probability of exceeding a certain EIFS (i.e. 1-P)

3.3 Crack growth curve

A phase-by-phase crack growth analysis was carried out by IMP Aerospace, which results are presented in Fig. 9. The analysis was performed using FASTRAN, and the presented curve combines crack path 1-2 and crack path 3-4. The hole diameter was simply added to crack path 3-4 after the crack path 1-2 had failed. A spectrum representing 15,000 hours was generated using the Service Life Assessment Program (SLAP) software: Database Interface/Spectra Sequencing Tool (DBI/SST) for the FASTRAN analysis. As required by the NRC risk analysis, the IMP crack growth analysis started from an initial crack size of 0.002 inch.

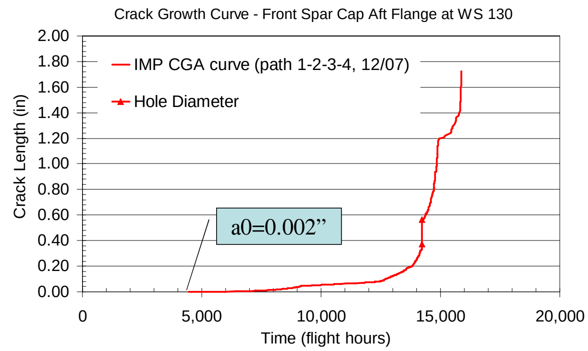

Fig. 9. Crack growth curve, combined from crack path 1-2 and 3-4.

As mentioned before, the crack growth curve for crack path 1-2 was used to regress the only crack finding (0.03” at 22,162 hours) to the EIFS. The regressed EIFS of 1.736×10^{-5} inch (or 0.04 μm) was found to be much smaller than previously observed material intrinsic discontinuities (crack-nucleating particles or pores) or manufacturing discontinuities (scratches, marks). This implies that the crack growth analysis is very conservative, especially in the small/short crack regime.

It should be noted that using the more accurate stress spectra generated from the strains recorded from the CP-140 Structural Data Recording Set (SDRS), the updated crack growth analyses predicted much longer fatigue lives for many CP-140 locations. Recently NRC also developed the stress intensity factor solutions to allow a simultaneously growth of crack paths 1-2 and 3-4 by accounting for the interaction of the two radial cracks [13], which was shown to provide more accurate crack growth analysis than the phase-by-phase crack growth analysis. For conservative POF study, this paper still used the original IMP crack growth curve based on the DBI/SST tool.

3.4 Stress exceedance data and maximum (peak) stress distribution

The stress exceedance data, as shown in Fig. 10, was generated by the P3 SLAP DBI/SST software for the 15,000-hour spectrum generated for this location. It was assumed that cracked structures fail under a maximum (peak tension) stress during a cyclic loading. Therefore, only the maximum stress data was used to determine a maximum stress (σ_{max}) distribution, i.e. the probability of exceeding a certain maximum stress value, per flight hour. Fig. 11 presents the σ_{max} data per flight hour, which was converted using the Berens approach [10]. A cutoff stress of 30 ksi at a probability of exceedance of 10^{-10} was added based on engineering judgment of the CF, IMP and NRC. These σ_{max} data can be directly used by the NRC tool ProDTA, or fitted with a Gumbel distribution (Type-I extreme value distribution of maxima) as,

$$H(\sigma_{max}) = Exp[-Exp((\sigma_{max} - B)/A)] \qquad (7)$$

where *A* and *B* are scale and location parameters of the Gumbel distribution. Based on the Berens' approach, the last five actual σ_{max} data points (except the last cutoff stress point) were used for the Gumbel fitting, resulting in A = 1.60, B = 14.69 ksi. Fig. 11 shows that the Gumbel distribution fitted the actual data very well, and it would give a higher (conservative) probability of exceeding than the actual data point when σ_{max} > 27ksi. Thus the Gumbel distribution, which was also used for the PoF calculation, was expected to result in conservative (higher) PoF results.

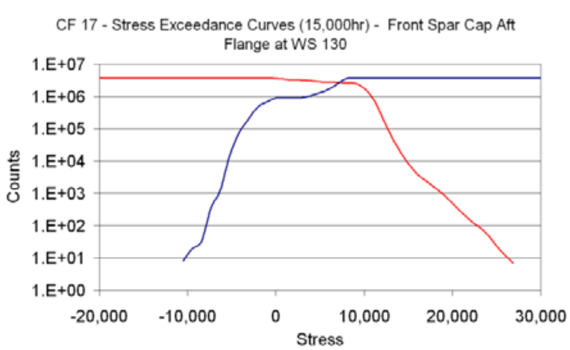

Fig. 10. Original stress exceedance curves for 15,000 flight hours

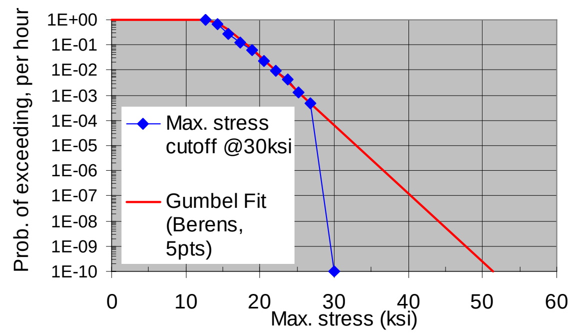

Fig. 11. Probability exceeding maximum stress (per flight hour) and Gumbel distribution fit

3.5 Residual strength

The failure scenario simulated in this work is a consecutive process with the first failure of the crack path 1-2 (reaches to the edge of the flange) and then the failure of the crack path 3-4. At first, the residual strength (RS) data, shown as data points in Fig. 12, were calculated by IMP separately for crack paths 1-2 and 3-4, based on a fracture toughness (Kc) criterion. The Kc value used was 51.5 ksi√in, which is a lower bound of the Kc distribution, and has an average of 71 ksi√in for the 7075-T6 spar cap with a thickness of ~ 0.1 inch. Assuming a 10% coefficient of variation (COV) for a Normal distribution of Kc, there would be less than 3-in-1000 Kc values which would be lower than the 51.5 ksi√in lower bound (about 3 standard deviations below the average).

Next, NRC combined the two RS curves together to represent the consecutive crack growth scenarios of crack paths 1-2 and 3-4, and considering the continuing damage growth of crack path 3-4. The continuing damage size was approximately calculated by growing an initial crack of 0.005" to the time when the crack path 1-2 reached the edge of the flange (edge failure). As shown in Fig. 12, the combined RS curve (line) is much lower than the starting RS strength of the crack path 3-4, which is expected to result in conservative (higher) PoF results.

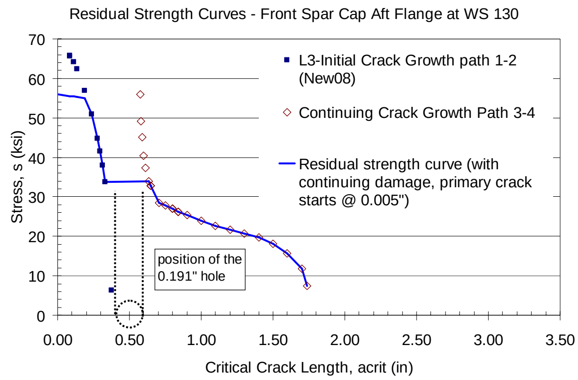

Fig. 12. Residual strength data and curve

3.6 POF results

Using the NRC in-house tool ProDTA, the SFPOF of Location 3 was calculated using the conservative Lincoln Eq. (2). The SFPOF (for crack path 1-2-3-4) are presented in Fig. 13 for two EIFSDs based on 1) $\sigma_{\log-TTCS}$ =0.103 (before TTCS regression) and 2) $\sigma_{\log-TTCS}$ =0.133 (after TTCS regression). It is shown that the EIFSD based on $\sigma_{\log-TTCS}$ =0.133 gave higher/ conservative PoF results.

According to the RARM risk index matrix (Fig. 1), the NRC POF results indicated a *low* risk index at the inspection time of 22,162 hours (SFPOF = 1.2×10^{-9} to 6.5×10^{-8} < 10^{-7}), and a *medium* risk index at the targeted operational lifetime of 24,500 hours (SFPOF = 1.5×10^{-7} to 2.1×10^{-6} < 10^{-5}) when *assuming* a 'Military aircraft-Hazard Probability' and a 'Hazard Severity-Category B (Hazardous)' for the analyzed Location 3③, if without future inspection/repair interference. It should be noted that the formal risk acceptance or decision would be granted by technical and operational authorities, depending on the level of risk index. Overall, this paper intended to use this example to demonstrate a conservative POF study, given the conservative inputs, assumptions, and equations described in the above sections.

③ The full scale fatigue test showed that with much larger crack size (3~4 inches) or completely severed spar cap, while the wing had no catastrophic failure.

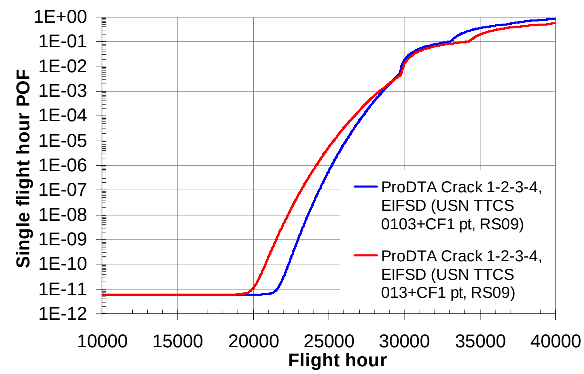

Fig. 13. Single flight hour PoF results for Location 3, using the two EIFSD derived from $\sigma_{\log-TTCS}$ =0.103 and 0.133 (before and after TTCS regression)

More POF results are presented in Fig. 14 to show the effect of the number of inspected holes on the POF results. As provided by IMP, the percentile for one crack found in 396 holes is *p**=1/396=0.25%. If there was a 20% variation on the number of holes inspected, the varied case would be *p**=1/320=0.31%. This variation could affect the EIFSD determined in this report and then the PoF result. However, Fig. 14 shows that this effect would be insignificant.

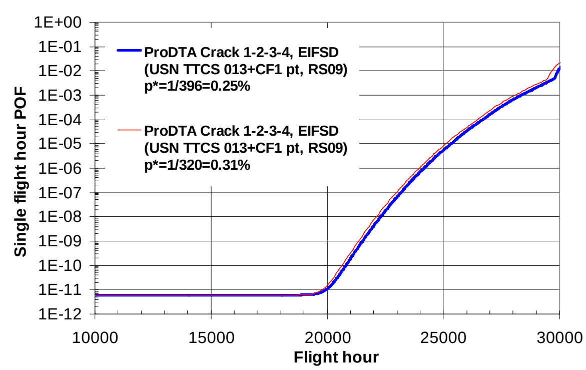

Fig. 14. Single flight hour POF results for Location 3 based on the different number of holes inspected

4 Discussions

It should be noted that this NRC POF study covered only one wing location; but it still provided additional support for the CF to downgrade the risk level of the wing structures to medium, which was largely based on the QETE inspection and IMP analyses. This case study demonstrated a conservative POF study using the limited in-service damage, which may be applied for other critical locations. Of course, for an entire wing or aircraft risk assessment, other damage findings, such as cracks on other wing locations, corrosion, hole elongation, and mechanical damage, would have to be taken into account. The follow-on inspection and repair, as well as the potential mechanical damages induced during these actions should also be taken into account in a risk assessment.

With more and more data and experience being accumulated for structural risk analysis, a *quantitative* risk analysis can be performed faster and easier, like an extended DTA. For example, with more accurate stress spectra available for many critical locations from the CP-140 SDRS system, the *quantitative* risk analyses can be quickly updated with more accurate crack growth curves. On the other hand, as more accurate SDRS based stress spectra have resulted in longer fatigue crack growth lives, it is justified that significant benefits can be gained from loads monitoring in a structural health monitoring (SHM) system.

5 Conclusions

A brief review of the CF RARM process shows that the risk assessment is becoming a very important tool for managing aircraft airworthiness. For complex structural systems, both *qualitative* and *quantitative* risk assessments are needed to support a decision-making.

A critical review of the different SPPOF definitions and calculations showed that the commonly used Lincoln SFPOF equation is more conservative than the exact Freudenthal equations. It would be useful to establish a standard SFPOF definition and calculation in the controlled documents for aircraft structural risk analysis.

For a small aircraft fleet with limited number of in-service damage findings, it is very challenging to carry out a *quantitative* risk assessment. This paper presented several methods for preparing the most important input, the ICSD/EIFSD, for a *quantitative* risk assessment. One of the in-service damage based methods was demonstrated through a risk analysis case study on a CP-140 wing location. Although with a number of conservative assumptions and inputs, the *quantitative* risk analysis could downgrade the risk level for the analyzed location, which in turn provided additional confidence for the decision-making of the aircraft life-cycle management.

6 Acknowledgements

This work was performed with financial support from DRDC (Defense Research and Development Canada) and NRC (National Research Council Canada) through project 13pp: "***Integrated Structural Life Assessment Method for the CF Air Fleets***".

Thanks to Mr. C. Chris, Dr. M. Oore, Mr. Aaron Muise of IMP Aerospace for providing some input data and technical discussion, Capt. M. Tourand, Mr. Y. Caron, and Mr. J. Gaerke of DTAES/DND for discussion and review.

References

[1] Department of National Defense of Canada (July 2007) Technical Airworthiness Manual (TAM), Department of National Defense of Canada, Document no. C-05-005-001/AG-001, 530 p.

[2] Komorowski, J.P., Bellinger, N.C., Liao, M. and Fillion, A. (2007) Application of the Holistic Structural Integrity Process to Canadian Forces Challenges, Proceedings of the 2007 USAF ASIP conference.

[3] Liao, M., Bellinger, N.C., Forsyth, D.S., and Komorowski, J.P., "A New Probabilistic Damage Tolerance Analysis Tool and its Application for Corrosion Risk Assessment", The 23rd Symposium of the International Committee on Aeronautical Fatigue, ICAF 2005, June 2005, Hamburg, Berlin, published by EMAS Publishing, pp 241-252.

[4] Liao, M., Bombardier, Y., Renaud, G., and Bellinger, N.C., "Advanced Damage Tolerance and Risk Assessment Methodology and Tool for Aircraft

Structures Containing MSD/WFD", The International Council of the Aeronautical Sciences (ICAS) 2010 Congress From 9/19/2010 To 9/24/2010, Nice, France.

[5] Department of Defense Standard Practice, “Aircraft Structural Integrity Program (ASIP)”, MIL-STD-1530C (USAF), Nov. 2005.

[6] United States of America Department of Defense, “Aircraft Structures” United States Department of Defense, JSSG-2006, 1998.

[7] United States of America Department of Defense, “Standard Practice for System Safety”, MIL-STD-882D, Feb. 2000.

[8] Liao, M., “Comparison of Different Single Flight Probability of Failure (SFPOF) Calculations for Aircraft Structural Risk Analysis”, The 2012 Aircraft Airworthiness and Sustainment (AA&S) Conference, Baltimore, USA, April 2-5, 2012 (http://www.airworthiness2012.com/)

[9] Lincoln, J. W., Risk assessment of an aging military aircraft, Journal of Aircraft, Vol. 22, No. 8, 1985, pp 687-691.

[10] Berens, A.P., Hovey, P.W., and Skinn, D.A., Risk analysis for aging aircraft, Vol.1 – Analysis, WL-TR-91-3066, Air Force Research Laboratory, Wright-Patterson Air Force Base, Ohio, 1991.

[11] Liao, M., Renaud, G., Bombardier, Y., and Bellinger, N.C., Development of Initial Crack Size Distribution for Risk Assessment of Aircraft Structures, NATO RTO Symposium AVT-157 on Ensured Military Platform Availability, Oct. 2008, Montreal, Canada

[12] Liao, M., Carey, C., Oore, M., and Tourond, M., “Quantitative risk assessment for CP-140 wing structures”, The 20th CASI Aircraft Design & Development Symposium, Kanata, Canada, May, 2009.

[13] Bombardier, Y., Liao, M., Renaud, G. “Modeling of Continuing Damage for Damage Tolerance Analysis”, Proceedings of the 2011 International Committee on Aeronautical Fatigue Symposium, Montréal, June 1-3 2011.

[14] Liao, M., Renaud, G., “Statistical Analysis for Assessing the CC-130 Centre Wing Service Life Limit”, LTR-SMPL-2011-0023, 2011.

Copyright Statement